Small G-Protein Rho Is Involved in the Maintenance of Cardiac Myocyte Morphology

Haslett R. Grounds, Dominic C.H. Ng, and Marie A. Bogoyevitch*

Biochemistry and Molecular Biology, University of Western Australia, Crawley,
Western Australia 6009, Australia

Abstract The use of small membrane-permeable sequences or protein transduction domains (PTDs) can facilitate the transport of proteins into many cell types. In preliminary studies with the application of three PTDs (penetratin, modified penetratin, and the HIV TAT transduction domains) to cardiac myocytes, we found that the TAT and penetratin sequences showed high efficiency of uptake and low toxicity. Rho has been previously shown to be an important regulator of cytoskeletal organization and morphology in other non-cardiac cell types. To evaluate a role for Rho in cardiac myocyte morphology, we used the TAT-PTD to deliver a RhoA-specific inhibitor, the C3 exoenzyme, to cultured cardiac myocytes. We showed that this incubation with TAT-C3 abolished the basal levels of RhoA activity, demonstrating the efficacy of this treatment. Incubation with TAT-C3 also altered cardiac myocyte morphology so that TAT-C3-treated cells produced multiple projections from the major cell body. This was accompanied by a statistically significant increase in cell size, albeit to a lesser extent than the changes accompanying exposure to the hypertrophic agent, endothelin-1. Furthermore, the change in size of TAT-C3-treated cells was not accompanied by the induction of atrial natriuretic factor (ANF) expression that accompanies the hypertrophy of cardiac myocytes. These results reveal a role for RhoA in the maintenance of normal myocyte morphology. J. Cell. Biochem. 95: 529–542, 2005. © 2005 Wiley-Liss, Inc.

Key words: cultured cardiac myocytes; protein delivery; small g-proteins; Rho; myocyte size; atrial natriuretic factor; myocyte morphology

The Rho family of small GTP-binding proteins (G-proteins) includes the protein subfamilies Rho (RhoA, RhoB, and RhoC), Rac, and Cdc42. In response to a variety of extracellular stimuli, these proteins are activated through their exchange of bound GDP with GTP. The resulting conformational changes trigger downstream signaling events culminating in the alteration of the actin cytoskeleton, changes in cell motility as well as specific upregulation of a subset of gene transcripts [see reviews Hall, 1998; Ridley, 2001; Boettner and van Aelst, 2002].

The specific function of RhoA in the myocytes of the heart under normal or pathological situations remains unclear. Hypertrophic stimuli including angiotensin II, mechanical stress, endothelin-1 (ET-1), phenylephrine, or lysophosphatidic acid rapidly increase the levels of GTP-bound RhoA in cultured myocytes [Aoki et al., 1998; Aikawa et al., 1999, 2000; Clerk et al., 2001; Hilal-Dandan et al., 2004]. Although this activated RhoA may mediate one or more aspects of the hypertrophic response of the cardiac myocyte, there is currently no agreement on the role(s) of cardiac RhoA. For example, Thorburn et al. [1997] suggested that Rho regulated gene expression but not the morphological changes upon phenylephrine stimulation. More recent studies have shown that RhoA activation influences the activities of members of the myocyte enhance factor 2 (MEF2) family of MADS-box transcription factors [Marinissen et al., 2001] as well as the GATA family of transcription factors [Yanazume et al.,

2002]. This is consistent with a role for RhoA as a regulator of gene transcription [Sah et al., 1996]. However, RhoA also regulates myofibril formation and organization in neonatal rat ventricular myocytes [Hoshijima et al., 1998].

Many studies examining the role of RhoA have used C3 exoenzyme, a bacterial toxin that is a high specificity inhibitor of the Rho subfamily of G-proteins [Aktories and Hall, 1989]. The mechanism of inhibition lies in the C3 catalyzed ADP-ribosylation of Rho proteins immediately adjacent to their GTP binding site and this prevents the interaction of Rho with exchange factors that promote its activation. In some of the first studies to evaluate the role of Rho proteins, the introduction of C3 into cells such as Swiss 3T3 fibroblasts or Vero cells via microinjection resulted in overall rounding of shape [Rubin et al., 1988; Chardin et al., 1989]. This suggested that Rho proteins play an important role in cytoskeletal arrangement.

Despite its specificity, C3 is devoid of the cell entry signals harbored by many other toxins. Although C3 may enter cells by non-specific pinocytosis, this is generally inefficient so invasive or labor-intensive procedures such as scrape loading, trituration, or microinjection have been used [Winton et al., 2002]. A recent solution to the delivery of C3 comes with the characterization of small membrane-permeable peptides known as "protein transduction domains" (PTDs). The first characterized PTD was derived from the human immunodeficiency virus 1 transcriptional activator TAT protein. When covalently coupled to other molecules, the TAT PTD sequence acts as an efficient vector for the delivery of small peptides (of <2 kDa) and biologically active proteins (of ∼120 kDa) [reviewed in Bogoyevitch et al., 2002]. Additional peptides including penetratin, derived from the *Drosophila* Antennapedia transcription factor, or modified penetratin, a synthetic variant of the original penetratin sequence, have also been shown to be efficient protein vectors [Bogoyevitch et al., 2002]. Despite the increasing use of PTD vectors, surprisingly few studies report their use in cardiac myocytes and perfused rat hearts [Chen et al., 2001, 2002; Gustafsson et al., 2002, 2004; Inagaki et al., 2003; Sugioka et al., 2003].

In this study, we demonstrate that the penetratin and TAT PTDs could be successfully used in cultured cardiac myocytes, showing high uptake and limited toxicity. We then used the TAT PTD as a delivery vector for the C3 exoenzyme and demonstrated uptake by a majority of the cultured myocytes, with subsequent lowering of basal RhoA.GTP levels. This was accompanied by an unusual alteration in cardiac myocyte morphology. Cells appeared larger and star-like in shape. Despite this increase in size, there was no increase in expression of the hypertrophic marker protein, atrial natriuretic factor (ANF). Thus, the use of TAT-C3 implicates RhoA in the maintenance of basal myocyte morphology.

MATERIALS AND METHODS

Chemicals and Reagents

Three biotinylated PTD peptides, TAT [sequence: (Biotin)-KGRRRQRRKKR], penetratin [sequence: (Biotin)-KKWKMRRNQFWI-KIQR], and "modified" penetratin [sequence: (Biotin)-KGRRWRRWWRRWWRRWRR] were synthesized by AUSPEP (Melbourne, Australia). Plasmid vectors for the bacterial expression of the glutathione *S*-transferase (GST)-fusion proteins (GST-Rhoketin and GST-TAT-C3 exoenzyme) were a gift from Dr. E. Sahai (Institute of Cancer Research, London). The protein assay reagent (#500-0006) was from Bio-Rad (Hercules, CA). Sera (horse as well as fetal bovine) for all cell culture work and streptavidin-FITC were from Invitrogen (Carlsbad, CA). Cell culture media (M199 and DMEM), gelatin, laminin, Endothelin-1 (ET-1), thrombin, *p*-aminobenzamidine-Sepharose, Phalloidin TRITC, and Hoescht 33258 were from Sigma-Aldrich (St. Louis, MO).

The monoclonal anti-RhoA antibody (clone 26C4) was from Santa Cruz Biotechnology (Santa Cruz, CA), and the monoclonal anti-rat ANF antibody (cat. no. IHC 9103) was from Peninsula Laboratories, Inc./Bachem Bioscience, Inc. (King of Prussia, PA). The anti-myc epitope antibody (clone 9E10) and the Annexin V-FLUOS staining kit were from Boehringer Mannheim Corporation/Roche Applied Science (Indianapolis, IN). Secondary antibodies were either conjugates with horseradish peroxidase for immunoblotting (PIERCE, Rockford, IL) or Alexa Fluor 488 for immunostaining (Molecular Probes, Eugene, OR). Lumilight PLUS Chemiluminescent Substrate was also from PIERCE. Vectashield mounting medium was from Vector Laboratories (Burlingame, CA).

Preparation of Recombinant Proteins

GST-Rhotekin and GST-TAT-C3 [Sahai and Marshall, 2002] were expressed in the BL21 DE3 pLys^s *Escherichia coli* strain. Purified GST-Rhotekin protein was used without modification in the assessment of RhoA activation, whereas the GST-TAT-C3 protein was subjected to overnight cleavage with thrombin, allowing the purification of TAT-C3. Thrombin was then removed by the addition of *p*-aminobenzamidine-Sepharose. Protein purity was confirmed by SDS–PAGE analysis and Coomassie Blue staining. The proteins were stored in aliquots at −80°C prior to use.

Preparation and Treatment of Isolated Neonatal Rat Cardiac Myocytes

Cardiac ventricular myocytes were isolated from neonatal rats as previously described [Ng et al., 2001]. Cells were then plated on 60 mm dishes (4×10^6 cells) to perform biochemical assays and phase contrast microscopy studies or on 25 mm × 25 mm glass coverslips in 35 mm dishes (1×10^6 cells) for confocal microscopy studies. Prior to plating, 60 mm dishes had been precoated with 1 ml of 1% (w/v) gelatin solution for 5 min and then dried at room temperature in the laminar flow hood for a minimum of 10 min. Similarly, the coverslips were first washed in 1% (v/v) HCl for 20 min, washed in double deionized water, flame sterilized, and then 100 μl of ice-cold laminin solution [500 nM in phosphate-buffered saline (PBS)] was applied to each coverslip for 20 min prior to removing and drying in the laminar flow hood for a minimum of 20 min. Myocytes were then cultured in Dulbecco's Modified Eagle Medium (DMEM)/ Medium 199 (M199) (4:1) containing 10% (v/v) horse serum, 5% (v/v) fetal calf serum (FCS), and penicillin/streptomycin (100 U/ml) for ∼40 h before treatment. The cardiac myocytes were exposed to the C3 exoenzyme by directly adding the purified TAT-C3 fusion protein into the media at the required concentration (200 nM unless otherwise indicated) after overnight incubation of the cells in serum-free medium. Cells were incubated with TAT-C3 for up to 48 h.

Cell Lysis and Assay of Rho Activation

Following treatment, the culture media was removed and the cells were washed twice in ice-cold PBS. Cells were then lysed in 200 μl of 50 mM Tris-HCl pH 7.2, 500 mM NaCl, 5 mM MgCl$_2$, and 1% (v/v) Triton X-100 supplemented just before use with 1 mM Dithiothreitol (DTT), 20 μg/ml leupeptin, 20 μg/ml aprotinin, 100 μg/ ml phenylmethylsulfonylfluoride (PMSF), and 100 μg/ml Na$_3$VO$_4$. The resulting cell lysate was then vortexed and centrifuged (4°C, 10,000g, 10 min) to remove cell debris. The supernatant was then collected and analyzed further.

The binding of activated Rho (RhoA.GTP) to its effector Rhotekin was used to assess RhoA activation. GST-Rhotekin was immobilized on Glutathione Sepharose beads, and then washed three times before incubation with the cell lysate (30 min, 4°C, end-over-end mixing) to allow the binding of activated RhoA. The samples were then centrifuged and quickly washed twice before the addition of 10 μl of 3× concentrated SDS sample buffer. Samples (lysates or Rhotekin-bound proteins) were then separated by SDS–PAGE. Proteins were transferred to nitrocellulose and immunoblotted with antibodies to RhoA [1/100 in Tris-buffered saline containing 0.1% (v/v) Tween 20 and 5% (w/v) milk powder]. RhoA was detected with the enhanced sensitivity chemiluminescent substrate, Lumilight PLUS. Quantitation used a LAS1000 Lumi-imager to capture images and detect relative signal intensities.

Microscopy

Cardiac myocytes cultured on gelatin-coated dishes and exposed to TAT-C3 were examined by phase contrast microscopy. For further analysis by confocal scanning microscopy, cardiac myocytes were cultured on coverslips, subjected to experimental treatments, and then rinsed twice in ice-cold PBS. Following fixation with 4% (w/v) paraformaldehyde and permeabilization with 0.2% (v/v) Triton X-100 in PBS, myocytes were washed in Wash Buffer [0.5% (w/ v) BSA; 0.1% (w/v) glycine in PBS] and blocked with 5% (v/v) FCS in Wash Buffer (60 min; room temperature). Cells were then incubated in streptavidin-FITC (1/5000 in 5% FCS in Wash Buffer, 60 min, room temperature) to detect the uptake of biotinylated peptides, or with anti-myc clone 9E10 [1/500 in 5% (v/v) FCS in Wash Buffer; overnight; 4°C], followed by Alexa Fluor 488-labeled secondary antibody [1/300 in 5% (v/ v) FCS in Wash Buffer; 60 min; room temperature] to detect the uptake of myc-TAT-C3.

Cell morphology and size were visualized through the staining of the actin-containing

myofilaments with phalloidin-TRITC [0.2 μg/ml in 5% (v/v) FCS in Wash Buffer; 60 min, 37°C]. ANF staining was also performed on these cells and used the anti-ANF antibody [1/100 in 5% (v/v) FCS in Wash Buffer; 60 min; room temperature] followed by Alexa Fluor 488-labeled secondary antibody [1/300 in 5% (v/v) FCS in Wash Buffer; 60 min; room temperature]. Cell nuclei were then stained with Hoechst 33258 (2 μg/ml; 5 min; room temperature). Stained cells were viewed using the Bio-Rad MRC 1000/1024 UV Scanning Confocal Microscope and acquired images subjected to Kalman filtering (3 scans) to reduce image noise.

To distinguish normal cardiac myocytes from those either undergoing apoptosis or necrosis or those permeabilized non-specifically by the PTDs, unfixed cardiac myocytes were stained with Annexin V-FITC and propidium iodide (PI) according to the manufacturer's instructions (Boehringer Mannheim Corporation). Briefly, cardiac myocytes cultured on laminin-coated glass coverslips were washed twice in ice-cold PBS, and then each coverslip was mounted on to a customized stage for live cell viewing by confocal microscopy. The cells were then stained for 15 min with 2% (v/v) Annexin V-FITC labeling reagent, 1 μg/ml PI in 10 mM Hepes pH 7.4, 140 mM NaCl, and 5 mM $CaCl_2$. Following a further one in four dilution of the labeling solution, the fluorescence of Annexin V-FITC and PI were visualized by confocal microscopy.

Image Analysis

Using confocal microscopy, fields containing between 30 and 50 cells were selected. Total cell number was estimated from the number of cell nuclei, and then the numbers of ANF positive cells were counted. Typically 200 cells per sample were counted in total for each sample and the results expressed as a percentage of ANF positive cells. In parallel, images of phalloidin-stained cells were captured and cell areas from these images were determined using Image Pro Plus (Media Cybernetics, Silver Spring, MD). Typically, 5 confocal images containing between 10 and 20 cells were analyzed for each sample. The boundaries of myocytes were manually identified and the area within these cell boundaries was then calculated. Statistical analysis with 2-tailed, unpaired t-tests was performed using the program Statview TM SE + Graphics (Abacus Concepts, Inc., Berkeley, CA).

RESULTS

Use of PTDs in Cultured Cardiac Myocytes

Despite the increasing use of PTDs to deliver proteins, relatively few studies have used this approach to alter signal transduction pathways in cardiac myocytes [Chen et al., 2002, 2002; Gustafsson et al., 2002, 2004; Inagaki et al., 2003; Sugioka et al., 2003]. We first examined three PTDs previously well-characterized in other cell types [see review Bogoyevitch et al., 2002] for their uptake into cultured cardiac myocytes. As shown in Figure 1, when we examined control cardiac myocytes (Fig. 1a) or cardiac myocytes exposed to the biotinylated peptides, TAT (Fig. 1b), penetratin (Fig. 1c), or "modified" penetratin (Fig. 1d), all cells treated with peptides showed enhanced staining with streptavidin-FITC (open arrow heads). Whilst this may suggest the suitability of all three PTDs for use with cardiac myocytes, a closer examination revealed increased cell debris in cultures exposed to "modified" penetratin, but not the TAT or penetratin peptides (Fig. 1d, large arrow heads).

We then evaluated membrane permeability and viability of PTD-exposed cells examined in their live and unfixed state with the use of an Annexin V-FITC conjugate [Koopman et al., 1994]. Control cells showed limited staining with Annexin V-FITC (Fig. 2a, left panel) but there was increased staining in all PTD-treated cell cultures (Fig. 2b,d, left panels). Co-staining of these cells with the nuclear stain PI showed that only a small percentage of cells were PI positive following exposure to TAT (Fig. 2b, right panel), but this was greater with penetratin-exposure (Fig. 2c, right panel). Almost all nuclei were PI positive when the cells had been exposed to "modified" penetratin (Fig. 2d, right panel). Thus, TAT appeared as the most suitable vector, with lower toxicity than the penetratin or "modified" penetratin PTD.

PTD Delivery of C3—Use of TAT-C3 in Cultured Cardiac Myocytes to Inhibit RhoA

We were interested in evaluating the role that RhoA plays in normal cardiac myocytes. As shown in Figure 3a, we detected active, GTP-bound RhoA in untreated cardiac myocytes. This level of GTP-bound RhoA could be subsequently increased some four-fold upon short-term exposure to ET-1 (Fig. 3a). We next confirmed cytosolic staining of
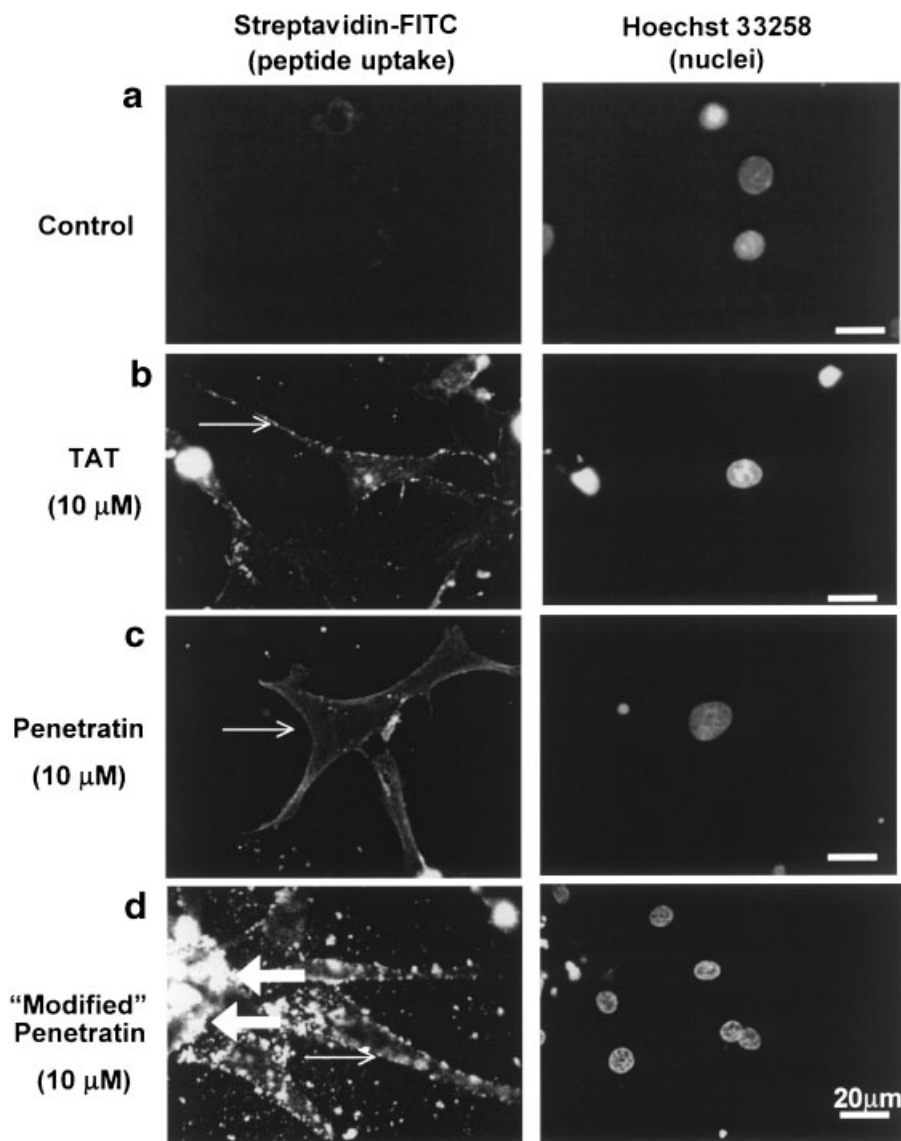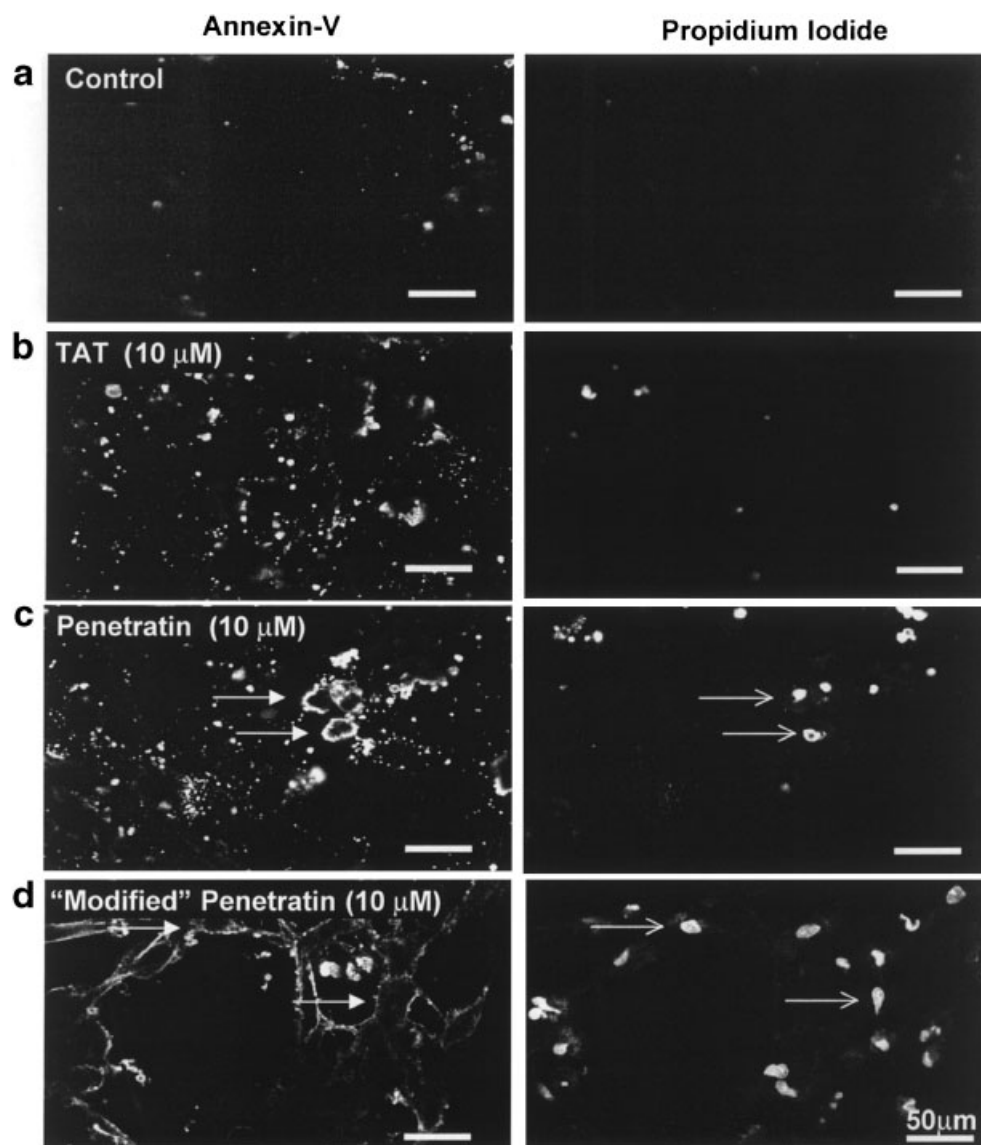
Fig. 1. Evaluation of the acute uptake of protein transduction domains (PTDs) in cardiac myocyte cultures. Cardiac myocytes were either left untreated as controls (**a**) or treated for 15 min with 10 μM FITC-labeled PTDs as follows: (**b**) TAT, (**c**) penetratin, or (**d**) ''modified'' penetratin. The presence of PTD intracellularly was determined by staining the cells with a streptavidin-FITC (**left panels**) and the presence of cells was confirmed by staining of nuclei with Hoescht 33258 (**right panels**). Cellular debris stained intensely with the streptavidin-FITC, especially following the treatment with modified penetratin, indicated that there was substantial association of the PTDs in this material (arrow heads in lowest panel). The staining of cellular membranes is indicated by open arrows in the **middle panels**. In all images, the scale bar = 20 μm. This was repeated on three independent occasions.

myocytes incubated with TAT-C3 (Fig. 3c,d) whereas no staining was observed for untreated cells (Fig. 3b). Importantly, TAT-C3 treatment led to the loss of active, GTP-bound RhoA over a 12 and 24 h incubation period (Fig. 3e). This is consistent with the loss of basal Rho activity in PC12 cells treated with TAT-C3 for 24 h [Winton et al., 2002].

TAT-C3 Exposure Changes Cardiac Myocyte Morphology, Leads to Myocyte Enlargement but Does not Alter ANF Expression

Given the well-documented role of Rho in regulation of the organization of actin in the cytoskeleton, together with the controversy surrounding the role of Rho in cardiac myocyte

Annexin-V   **Propidium Iodide**

Fig. 2. Evaluation of the acute toxicity of protein transduction domains (PTDs) in cardiac myocyte cultures. Cardiac myocytes were either left untreated as controls (**a**) or treated for 15 min with (**b**) TAT, (**c**) penetratin, or (**d**) ''modified'' penetratin. Unfixed, unpermeabilized cardiac myocytes were stained with a combination of Annexin-V (shown in the **left panels**) and the nuclear stain propidium iodide (PI; shown in the **right panels**). Annexin V associates with plasma membranes of either leaky or apoptotic cells (indicated by solid arrow heads), whereas PI only stains the nuclei of cells that it enters through leaky/ruptured membranes (indicated by open arrow heads). In all images, the scale bar = 50 μm. This was repeated on three independent occasions.

Fig. 3. Validation of the uptake and actions of TAT-C3 exoenzyme in cultured cardiac myocytes. **a:** Cardiac myocytes were serum-starved and then treated with 100 nM ET-1 for 0–300 s. Total RhoA levels were determined by immunoblotting cell lysates for RhoA, and RhoA.GTP levels were determined by incubating cell lysates with GST-Rhotekin and then immunoblotting associated pellet for RhoA. The results were quantified by Lumi-imaging from three independent experiments and expressed as the relative activation of RhoA. To then assess the uptake efficiency of the TAT-C3 protein, cardiac myocytes were incubated (**b**) in the absence of TAT-C3 or (**c**) and (**d**) the presence of 200 nM TAT-C3. The inclusion of the myc epitope tag in the TAT-C3 protein allowed for its detection using an anti-myc antibody (1/50 dilution) followed by an ALEXA 488-tagged secondary antibody (1/300 dilution; red). Nuclei were stained with Hoescht 33258 (blue) in panels (b) and (c). In panels (b) and (c), the scale bar = 100 μm. In panel (d), the scale bar = 50 μm. **e:** The effects of TAT-C3 exposure on the levels of active Rho (RhoA.GTP) were confirmed by incubating cell lysates with GST-Rhotekin and then immunoblotting associated pellet for RhoA. Total RhoA levels confirmed comparable loading under these conditions. This was repeated on three independent occasions. [Color figure can be viewed in the online issue, which is available at www.interscience.wiley.com.]
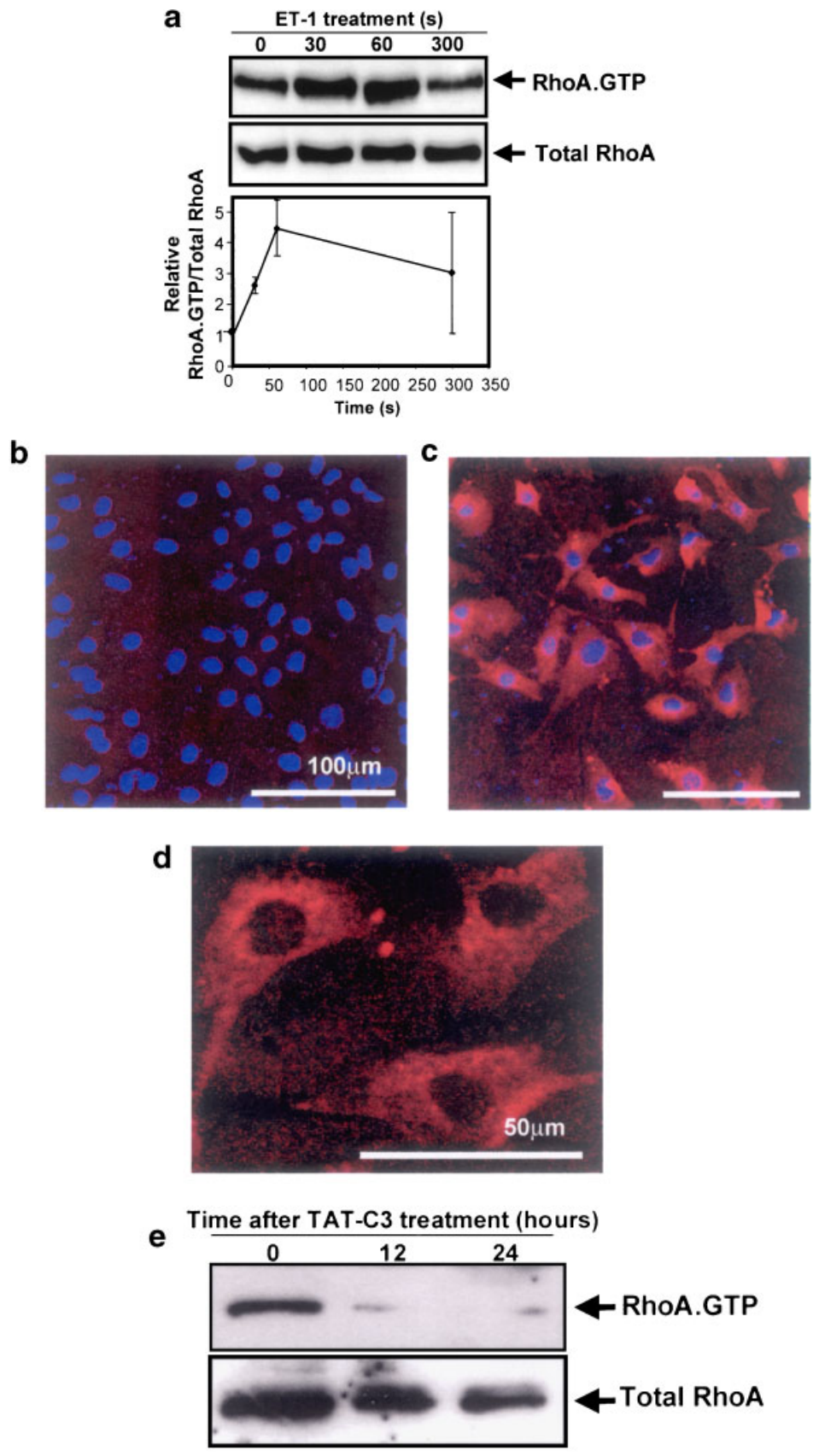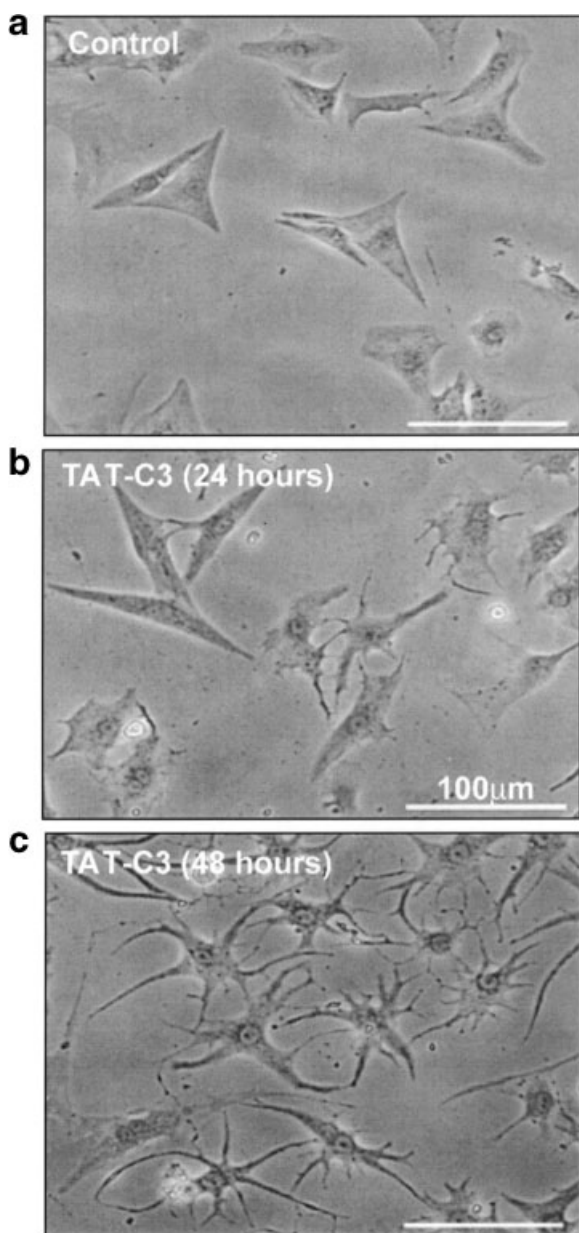
Fig. 3.

morphology and gene expression, we next evaluated the long term consequences of culturing cardiac myocytes in the presence of 200 nM TAT-C3. As shown in Figure 4a, control myocytes appeared regular in shape, but during 24–48 h of culture in the presence of TAT-C3, myocytes developed multiple projections, ultimately becoming more star-like in appearance (Fig. 4b,c). To our knowledge, this is the first report of this morphological change in cardiac myocytes. This contrasts the recent observation that the application of C3 (40 µg/ml, equivalent to 1.6 µM assuming a molecular weight for C3 of 25 kDa, for 16–18 h prior to exposure to lysophosphatidic acid) without conjugation to the TAT-PTD did not cause any changes in the morphology of cultured cardiac myocytes [Hilal-Dandan et al., 2004].

The morphological changes under our experimental conditions were further examined by the staining of cultured cardiac myocytes for actin using phalloidin-TRITC. As shown in Figure 5a,b, the change in myocyte morphology to a more star-like appearance for TAT-C3-treated myocytes was observed when examined under confocal scanning microscopy at low magnification. This contrasted with the morphological changes accompanying exposure to the hypertrophic agent ET-1 (Fig. 5c). The size of 50 myocytes per treatment was evaluated on three independent occasions. This showed an increase in the area of at least 25% ($P < 0.001$, 2-tail unpaired t-test) when control cells (Fig. 5a) were compared with TAT-C3-treated cells (Fig. 5b). However, this was lower than the 200% increases in size when cells were treated with ET-1 ($P < 0.0001$, 2-tail unpaired t-test). In the lower panel of Figure 5c, an ET-1-treated myocyte of size similar to the TAT-C3-treated cell shown in Figure 5b is shown to facilitate the comparison of cell morphologies.

An evaluation of individual myocytes at these higher magnification also showed actin in organized structures consistent with sarcomeric organization in both the control, TAT-C3-treated, or ET-treated myocytes, and that for the TAT-C3-treated cells these sarcomeric structures extended into the longer projections (Fig. 5b lower panel). We also examined the expression of ANF in control cells and those treated with TAT-C3 by immunostaining cells for ANF and calculating the percentage of ANF positively-staining cells following each treatment. Less than 10% of the cells stained positive for ANF expression following TAT-C3 treatment, and this contrasted with >60% ANF positive cells following ET-1 treatment. Thus, ANF expression was not
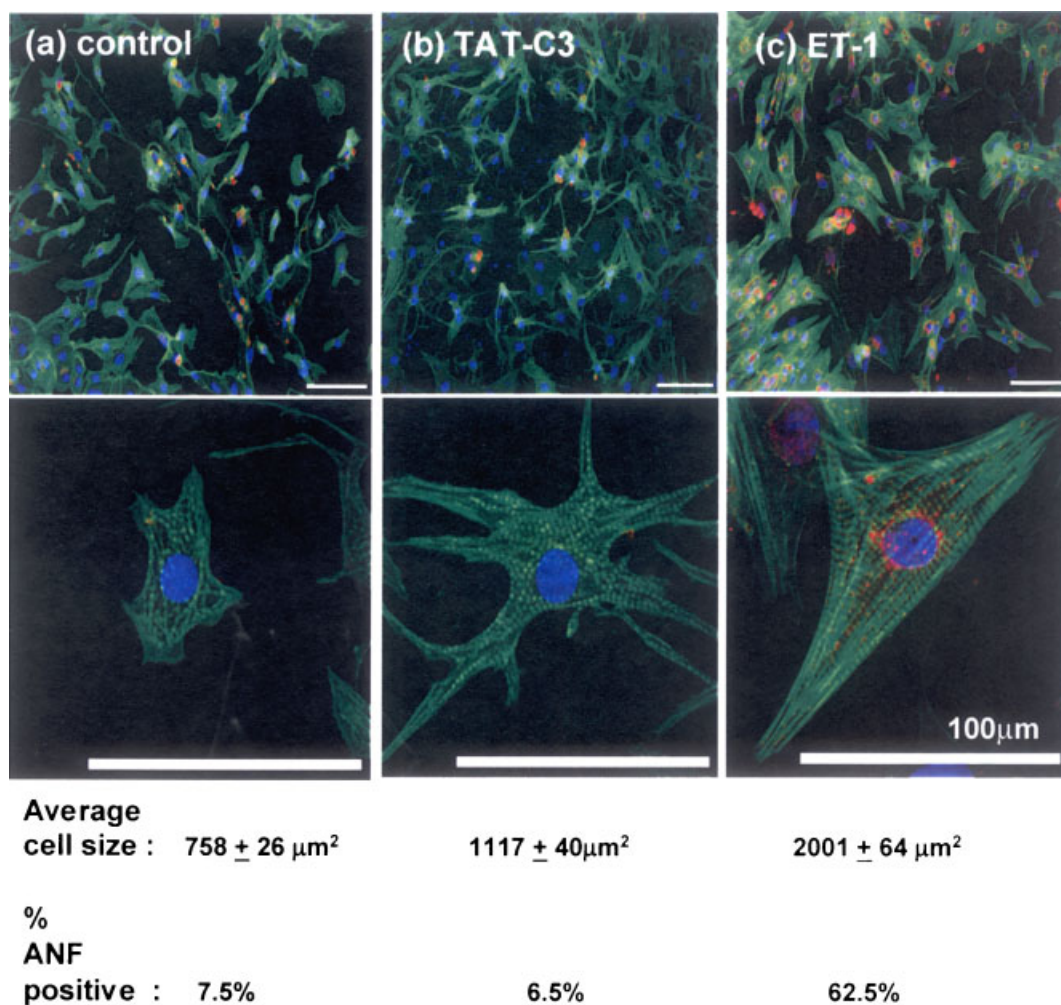

Fig. 4. Phase contrast microscopy reveals prolonged TAT-C3 exposure leads to altered cardiac myocyte morphology. Cardiac myocytes were serum-starved and then treated with 200 nM TAT-C3 for (**b**) 24 h or (**c**) 48 h, or (**a**) left untreated during the 48 h period. Live, unfixed cells were viewed under phase contrast to assess morphological changes and toxicity of TAT-C3 exposure. In all images, the scale bar = 100 µm. TAT-C3 exposure for 48 h showed maximal morphological differences, however, some myocytes showed more subtle stellate-morphologies within the first 24 h of exposure. This was observed on more than six independent occasions.

Fig. 5. Confocal scanning microscopy reveals prolonged TAT-C3 exposure leads to altered cardiac myocyte morphology and increased cell size, but no change in ANF-positive cells. Cardiac myocytes were (**a**) serum-starved under control conditions, (**b**) treated with TAT-C3 (200 nM) for 48 h, or (**c**) treated with 100 nM Endothelin-1 (ET-1) for 48 h as a positive control. Fixed cells were stained for ANF expression (red) or actin myofilaments using phalloidin (green), and Hoescht 33258 stain (blue) identified the nuclei. In all images, the scale bar = 100 μm. From the images acquired, 200 cells were assessed and the average cell size and percentage ANF positive were calculated. [Color figure can be viewed in the online issue, which is available at www.interscience.wiley.com.]

increased in cells treated with TAT-C3 as it was in ET-1-treated cells despite the increase in size of the TAT-C3-treated or ET-1-treated cells.

We confirmed that the changes in cell shape were not due to the inclusion of GST (Fig. 6b) or TAT alone (Fig. 6c) in the cell culture media. Inclusion of C3 alone (Fig. 6d) produced a similar but less robust change in cell shape (Fig. 6e) when compared to those cells treated with TAT-C3 (Fig. 6f). This result may explain the difference in results obtained when using TAT-C3 or C3 alone as in the study of Hilal-Dandan et al. [2004]. We also confirmed that the changes were dependent on the dose of C3

(Fig. 7). Specifically, 10 nM TAT-C3 did not alter cell morphology (Fig. 7b), whereas 100 nM TAT-C3 resulted in the star-like morphology (Fig. 7c). As the dose of TAT-C3 was then progressively increased to 2 μM, signs of cell toxicity were apparent (Fig. 7e,f). We have noted similar problems with toxicity with the culture of myocytes in the presence of TAT alone at micromolar concentrations when incubation times continue for more than 24 h (results not shown). This contrasts the limited toxicity we observed with incubation in the presence of 10 μM TAT for short periods of time such as the 15 min incubation shown in Figure 1b.
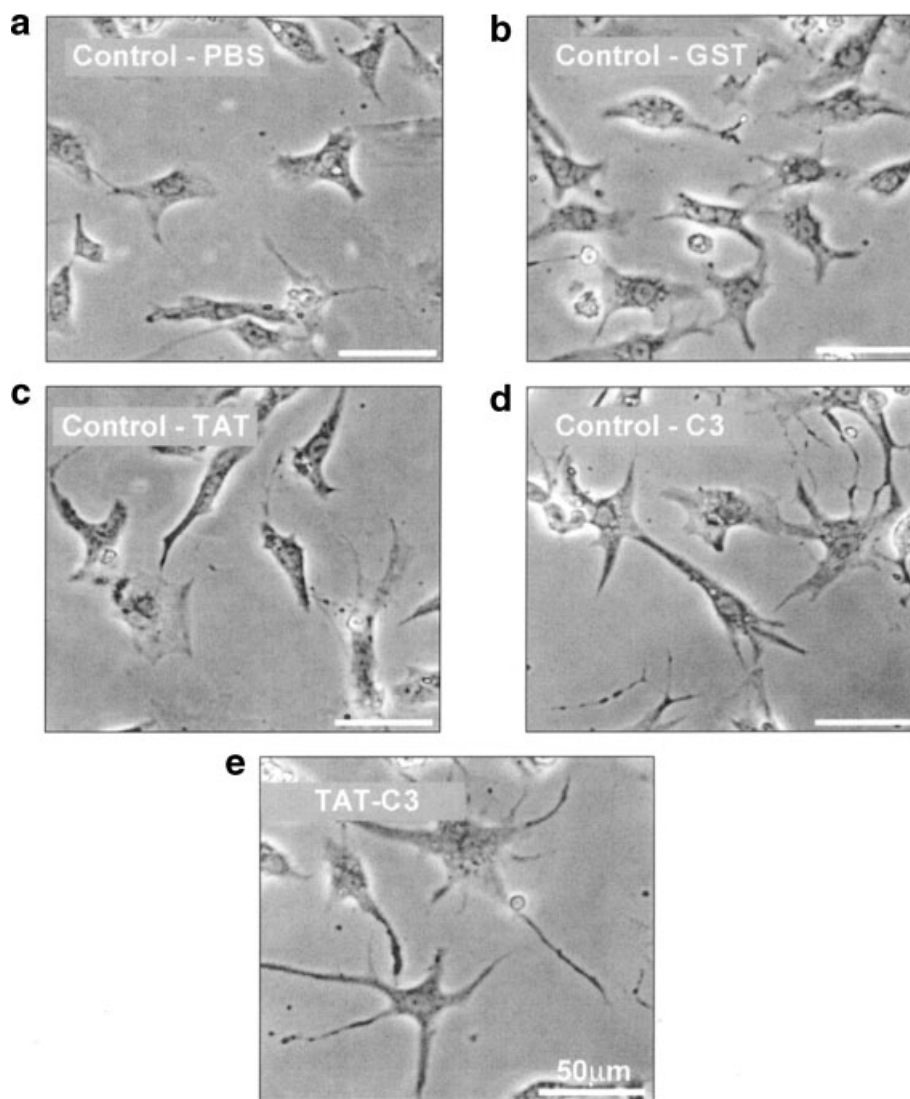
Fig. 6. Control experiments confirm that TAT-C3 is required for the morphological changes. Cardiac myocytes were (**a**) serum-starved under control conditions or treated for 48 h with (**b**) 200 nM GST prepared under the conditions used to prepare TAT-C3, (**c**) 200 nM TAT only, (**d**) 200 nM C3 only, or (**e**) 200 nM TAT-C3. Live, unfixed cells were viewed under phase contrast to assess morphological changes following treatment. In all images, the scale bar = 50 μm. TAT-C3 exposure for 48 h showed maximal morphological differences, however, some myocytes showed more subtle stellate-morphologies following exposure to C3 alone but not in response to TAT alone or GST alone. This was observed on three independent occasions.

DISCUSSION

Studies in which the activated form of the small G-protein Ras was overexpressed under the control of the ventricular myosin light chain-2 promoter provided some of the first and most compelling evidence that small G-proteins could play a role in the development of cardiac hypertrophy [Hunter et al., 1995; Gottshall et al., 1997]. Indeed, the activation of Ras by the receptors for a diverse range of hypertrophic stimuli provides a link between the early signaling events and the hypertrophic processes [Sugden and Clerk, 2000]. Similarly, some hypertrophic stimuli can also activate the small G-protein RhoA [Clerk and Sugden, 2000] suggesting that this small G-protein may also be a critical regulator in the signal transduction events regulating hypertrophy. However, when transgenic animals with cardiac-specific overexpression of RhoA have also been generated and then examined, the changes in the heart were more complex, with progressive left ventricular dilatation and associated decreases in left ventricular contractility [Sah et al., 1999].
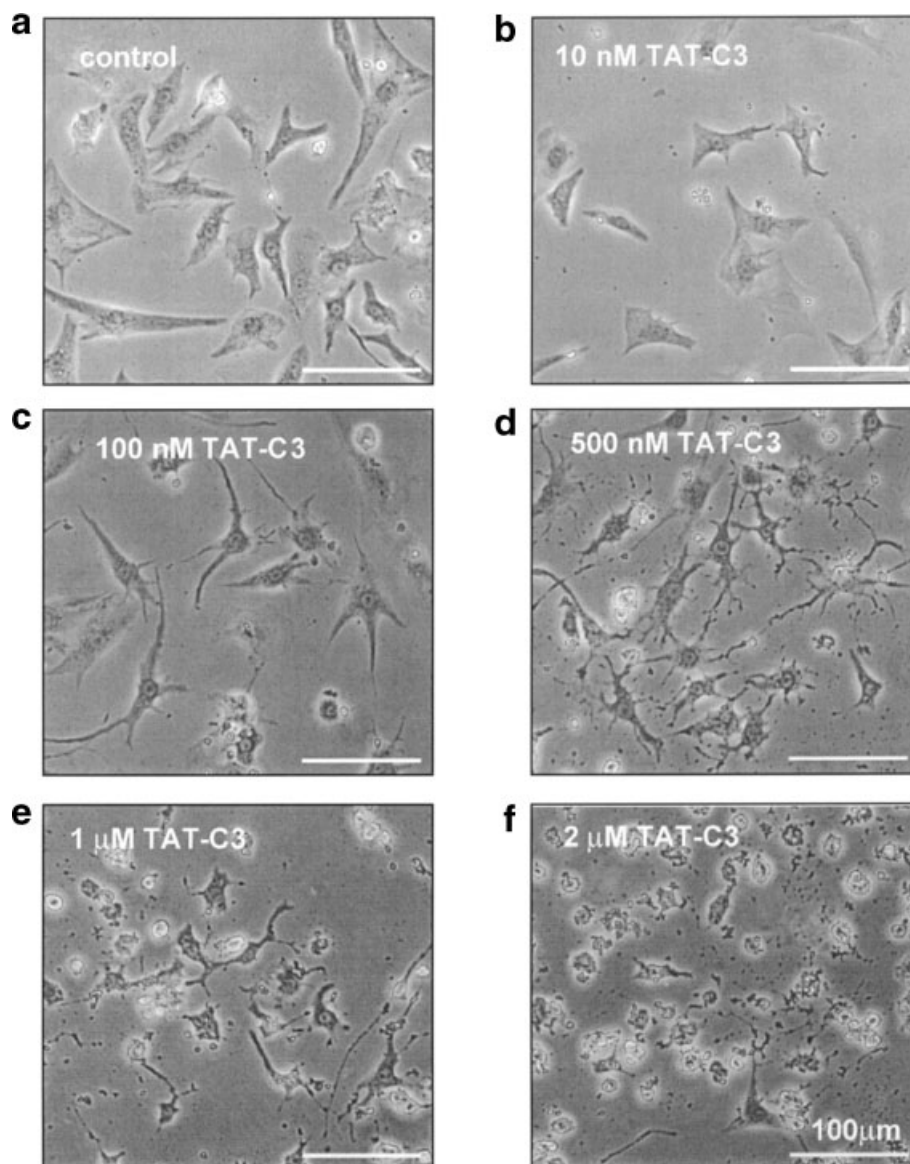
Fig. 7. Dose response effects of TAT-C3 treatment reveal toxicity at higher doses. **(a)** to **(f)** Cardiac myocytes were serum-starved and then treated with TAT-C3 at the indicated doses (0–2 μM) for 48 h. This contrasts the short-term exposures shown in Figures 1 and 2. Live, unfixed cells were viewed under phase contrast to assess morphological changes and toxicity of TAT-C3 exposure. In all images, the scale bar = 100 μm. TAT-C3 concentrations between **(a)** 0 and **(b)** 10 nM caused no changes in morphology. TAT-C3 concentrations between **(c)** 100 and **(d)** 500 nM showed maximal morphological differences with concentrations exceeding 500 nM **(e)** and **(f)** showing marked toxicity as evidenced by the loss of adherent cells and increased cellular debris. This was observed on three independent occasions.

These overexpression studies indicate possible outcomes when activation levels of the small G-proteins are high and maintained for long periods of time. An alternative approach to evaluate the participation of small G-proteins requires their inhibition. In cardiac myocytes this has been achieved with transfection of cultured cardiac myocytes with inactive RhoA mutants. This approach has implicated RhoA in hypertrophy stimulated by phenylephrine [Sah et al., 1996; Aoki et al., 1998]. Others have used C3, but not linked to a cell-permeable vector, and suggested that this can inhibit ANF expression induced by phenylephrine or angiotensin II [Sah et al., 1996; Thorburn et al., 1997; Aoki et al., 1998; Hines and Thorburn, 1998]. In those studies ANF expression was determined by reporter gene analysis or Northern blot analysis, both of which assess ANF transcript regulation/levels rather than ANF protein

levels. Furthermore, whilst some studies have suggested that application of C3 to myocytes can inhibit the formation of sarcomeric structures [Aoki et al., 1998; Hoshijima et al., 1998], others have not observed these same effects [Thorburn et al., 1997], and there is an implication of a related small G-protein Cdc42 in the serial assembly of sarcomeres [Nagai et al., 2003]. The reason for such disparate findings on the involvement of Rho in these processes has remained unknown although it may reflect the levels of C3 entering the cells under the different conditions.

To circumvent possible problems with delivery, we chose to evaluate the effects of the C3 exoenzyme produced as a recombinant fusion protein tagged by the PTD of the HIV Tat protein. This strategy has been used successfully in study of epithelial cell junctions [Sahai and Marshall, 2002], arterial smooth muscle contraction, actin stress fiber formation, and proliferation [Sauzeau et al., 2001] and implicating Rho as a negative regulator of neurite outgrowth [Winton et al., 2002]. Surprisingly, few studies have adopted the use of PTDs in the study of signal transduction in cardiac myocytes, but these have shown the success of the technique in delivery to both cultured cardiac myocytes [Chen et al., 2001] and the perfused heart [Chen et al., 2001, 2002; Gustafsson et al., 2002, 2004; Inagaki et al., 2003; Sugioka et al., 2003], and has the potential to act in vivo [Schwarze et al., 1999]. Here we have used PTD methodology to deliver a Rho inhibitor protein, the C3 exoenzyme, to myocytes. The observed effects implicate Rho in the maintenance of normal morphology of cardiac myocytes. This is the first study to our knowledge that has shown striking effects of Rho inhibition on the cardiac myocyte in the absence of hypertrophic stimulation [Aoki et al., 1998]. If we consider the recent study by Hilal-Dandan and colleagues, the incubation of cultured cardiac myocytes with an unconjugated C3 resulted in no observable effects on basal morphology [Aoki et al., 1998; Hilal-Dandan et al., 2004]. This agrees with the minimal effects on basal morphology that we observed when also using unconjugated C3. It may therefore be that the mode of delivery of C3 to these cells may influence the morphological outcome. This may reflect the intracellular concentrations of C3 achieved and thus the level of Rho inhibition achieved, or more complex events such as the kinetics of internalization and the subsequent kinetics of Rho inhibition, or possibly subcellular compartmentation of the different forms of C3 resulting in differential Rho inhibition.

The question remains on the mechanism underlying the changes in morphology of the myocytes in the presence of TAT-C3. Various exchange factors for Rho activation have been observed at the sarcomere of cardiac or striated muscle [Arai et al., 2002; Souchet et al., 2002], however, the predominant pool of Rho in cardiac myocytes appears not to be associated with the sarcomeres themselves [Sah et al., 1996]. Indeed, gross changes in the sarcomeric staining of actin were not observed in our study either in TAT-C3-treated control myocytes or ET-1-treated myocytes. There have been a number of reported differences in cell morphology following Rho inhibition, although ours is the first study to show these changes in cardiac myocytes. Thus, it has been noted that cell body contraction is dependent on Rho. For example, when Rho is inhibited by C3 microinjection into macrophages, these cells continue to extend processes, but the cell body does not translocate significantly [Allen et al., 1997, 1998]. In monocytes, inhibition of RhoA signaling also allows the formation of multiple competing lamellipodia [Worthylake and Burridge, 2003]. As recently reviewed by DeMali and Burridge [2003], a transient decrease in Rho activity initiated by β1-integrin engagement has been suggested to contribute to membrane protrusion, and conversely high Rho activity appears to antagonize membrane protrusion. The protein Smurf1 has also been shown to be involved in targeting RhoA for degradation during dynamic membrane movements [Wang et al., 2003]. Thus, the use of TAT-C3 as a direct and specific inhibitor of RhoA in cardiac myocytes suggests that the plasma membrane of each cardiac myocyte is a dynamic structure. It will, therefore, be of increasing interest to evaluate whether Rho-dependent movement of myocytes or changes in their morphology is of importance either in the normal heart under physiological conditions or whether this may contribute to the complex processes accompanying ischemia/reperfusion or longer term remodeling effects in the failing heart.

Paul Rigby for help with confocal scanning microscopy.

REFERENCES

Aikawa R, Komuro I, Yamazaki T, Zou Y, Kudoh S, Zhu W, Kadowaki T, Yazaki Y. 1999. Rho family small G proteins play critical roles in mechanical stress-induced hypertrophic responses in cardiac myocytes. Circ Res 84:458–466.

Aikawa R, Komuro I, Nagai R, Yazaki Y. 2000. Rho plays an important role in angiotensin II-induced hypertrophic responses in cardiac myocytes. Mol Cell Biochem 212: 177–182.

Aktories K, Hall A. 1989. Botulinum ADP-ribosyltransferase C3: A new tool to study low molecular weight GTP-binding proteins. Trends Pharmacol Sci 10:415–418.

Allen WE, Jones GE, Pollard JW, Ridley AJ. 1997. Rho, Rac and Cdc42 regulate actin organization and cell adhesion in macrophages. J Cell Sci 110:707–720.

Allen WE, Zicha D, Ridley AJ, Jones GE. 1998. A role for Cdc42 in macrophage chemotaxis. J Cell Biol 141:1147–1157.

Aoki H, Izumo S, Sadoshima J. 1998. Angiotensin II activates RhoA in cardiac myocytes. A critical role of RhoA in angiotensin II-induced premyofibril formation. Circ Res 82:666–676.

Arai A, Spencer JA, Olson EN. 2002. Stars, a striated muscle activator of Rho signaling and serum response factor-dependent transcription. J Biol Chem 277:24453–24459.

Boettner B, van Aelst L. 2002. The role of Rho GTPases in disease development. Gene 286:155–174.

Bogoyevitch MA, Kendrick TS, Ng DCH, Barr RK. 2002. Taking the cell by stealth or storm? Protein transduction domains (PTDs) as versatile vectors for delivery. DNA Cell Biol 21:879–894.

Chardin P, Boquet P, Madaule P, Popoff MR, Rubin EJ, Gill DM. 1989. The mammalian G protein rhoC is ADP-ribosylated by Clostridium botulinum exoenzyme C3 and affects actin microfilaments in Vero cells. EMBO J 8: 1087–1092.

Chen L, Wright LR, Chen CH, Oliver SF, Wender PA, Mochly-Rosen D. 2001. Molecular transporters for peptides: Delivery of a cardioprotective epsilonPKC agonist peptide into cells and intact ischemic heart using a transport system, R(7). Chem Biol 8:1123–1129.

Chen M, Won DJ, Krajewski S, Gottlieb RA. 2002. Calpain and mitochondria in ischemia/reperfusion injury. J Biol Chem 277:29181–29186.

Clerk A, Sugden PH. 2000. Small guanine nucleotide-binding proteins and myocardial hypertrophy. Circ Res 86:1019–1023.

Clerk A, Pham FH, Fuller SJ, Sahai E, Aktories K, Marais R, Marshall C, Sugden PH. 2001. Regulation of mitogen-activated protein kinases in cardiac myocytes through the small G protein Rac1. Mol Cell Biol 21:1173–1184.

Demali KA, Burridge K. 2003. Coupling membrane protrusion and cell adhesion. J Cell Sci 116:2389–2397.

Gottshall KR, Hunter JJ, Tanaka N, Dalton N, Becker KD, Ross J, Chien KR. 1997. Ras-dependent pathways induce obstructive hypertrophy in echo-selected transgenic mice. Proc Natl Acad Sci USA 94:4710–4715.

Gustafsson AB, Sayen MR, Williams SD, Crow MT, Gottlieb RA. 2002. TAT protein transduction into isolated perfused hearts: TAT-apoptosis repressor with caspase recruitment domain is cardioprotective. Circulation 106: 735–739.

Gustafsson AB, Tsai JG, Logue SE, Crow MT, Gottlieb RA. 2004. Apoptosis repressor with caspase recruitment domain protects against cell death by interfering with Bax activation. J Biol Chem 279:21233–21238.

Hall A. 1998. Rho GTPases and the actin cytoskeleton. Science 279:509–514.

Hilal-Dandan R, Means CK, Gustafsson AB, Morissette MR, Adams JW, Brunton LL, Heller Brown J. 2004. Lysophosphatidic acid induces hypertrophy of neonatal cardiac myocytes via activation of Gi and Rho. J Mol Cell Cardiol 36:481–493.

Hines WA, Thorburn A. 1998. Ras and Rho are required for Gα-induced hypertrophic gene expression in neonatal rat cardiac myocytes. J Mol Cell Cardiol 30:485–494.

Hoshijima M, Sah VP, Wang Y, Chien KR, Brown JH. 1998. The low molecular weight GTPase Rho regulates myofibril formation and organization in neonatal rat ventricular myocytes. Involvement of Rho kinase. J Biol Chem 273:7725–7730.

Hunter JJ, Tanaka N, Rockman HA, Ross J Jr, Chien KR. 1995. Ventricular expression of a MLC-2v-ras fusion gene induces cardiac hypertrophy and selective diastolic dysfunction in transgenic mice. J Biol Chem 270:23173–23178.

Inagaki K, Hahn HS, Dorn GW, Mochly-Rosen D. 2003. Additive protection of the ischemic heart ex vivo by combined treatment with delta-protein kinase C inhibitor and epsilon-protein kinase C activator. Circulation 108:869–875.

Koopman G, Reutelingsperger CP, Kuijten GA, Keehnen RM, Pals ST, van Oers MH. 1994. Annexin V for flow cytometric detection of phosphatidylserine expression on B cells undergoing apoptosis. Blood 84:1415–1420.

Marinissen MJ, Chiariello M, Gutkind JS. 2001. Regulation of gene expression by the small GTPase Rho through the ERK6 (p38 γ) MAP kinase pathway. Genes Dev 15: 535–553.

Nagai T, Tanaka-Ishikawa M, Aikawa R, Ishihara H, Zhu W, Yazaki Y, Nagai R, Komuro I. 2003. Cdc42 plays a critical role in assembly of sarcomere units in series of cardiac myocytes. Biochem Biophys Res Commun 305: 806–810.

Ng DCH, Long CS, Bogoyevitch MA. 2001. A role for the extracellular signal-regulated kinase and p38 mitogen-activated protein Kinases in Interleukin-1-stimulated delayed signal tranducer and activator of transcription 3 activation, atrial natriuretic factor expression, and cardiac myocyte morphology. J Biol Chem 276:29490–29498.

Ridley AJ. 2001. Rho family proteins: Coordinating cell responses. Trends Cell Biol 11:471–477.

Rubin EJ, Gill DM, Boquet P, Popoff MR. 1988. Functional modification of a 21-kilodalton G protein when ADP-ribosylated by exoenzyme C3 of Clostridium botulinum. Mol Cell Biol 8:418–426.

Sah VP, Hoshijima M, Chien KR, Heller Brown J. 1996. Rho is required for Gαq and a1-adrenergic receptor signaling in cardiomyocytes. Dissociation of Ras and Rho pathways. J Biol Chem 271:31185–31190.

Sah VP, Minamisawa S, Tam SP, Wu TH, Dorn GW, Ross J, Chien KR, Brown JH. 1999. Cardiac-specific overexpression of RhoA results in sinus and atrioventricular nodal dysfunction and contractile failure. J Clin Invest 103: 1627–1634.

Sahai E, Marshall CJ. 2002. Rock and Dia have opposing effects on adherens junctions downstream of Rho. Nat Cell Biol 4:408–415.

Sauzeau V, Le Mellionnec E, Bertoglio J, Scalbert E, Pacaud P, Loirand G. 2001. Human urotensin II-induced contraction and arterial smooth muscle cell proliferation are mediated by RhoA and Rho-kinase. Circ Res 88: 1102–1104.

Schwarze SR, Ho A, Vocero-Akbani A, Dowdy SF. 1999. In vivo protein transduction delivery of a biologically important protein into the mouse. Science 285:1569–1572.

Souchet M, Portales-Casamar E, Mazurais D, Schmidt S, Leger I, Javre JL, Robert P, Berrebi-Bertrand I, Bril A, Gout B, Debant A, Calmels TP. 2002. Human p63Rho-GEF, a novel RhoA-specific guanine nucleotide exchange factor, is localized in cardiac sarcomere. J Cell Sci 115: 629–640.

Sugden PH, Clerk A. 2000. Activation of the small GTP-binding protein Ras in the heart by hypertrophic agonists. Trends Cardiovasc Med 10:1–8.

Sugioka R, Shimizu S, Funatsu T, Tamagawa H, Sawa Y, Kawakami T, Tsujimoto Y. 2003. BH4-domain peptide from Bcl-xL exerts anti-apoptotic activity in vivo. Oncogene 22:8432–8440.

Thorburn J, Xu S, Thorburn A. 1997. MAP kinase- and Rho-dependent signals interact to regulate gene expression but not actin morphology in cardiac muscle cells. EMBO J 16:1899–1900.

Wang HR, Zhang Y, Ozdamar B, Ogunjimi AA, Alexandrova E, Thomsen GH, Wrana JL. 2003. Regulation of cell polarity and protrusion formation by targeting RhoA for degradation. Science 302:1775–1779.

Winton MJ, Dubreuil CI, Lasko D, Leclerc N, Mckerracher L. 2002. Characterization of new cell permeable C3-like proteins that inactivate Rho and stimulate neurite outgrowth on inhibitory substrates. J Biol Chem 277: 32820–32829.

Worthylake RA, Burridge K. 2003. RhoA and ROCK promote migration by limiting membrane protrusions. J Biol Chem 278:13578–13584.

Yanazume T, Hasegawa K, Wada H, Morimoto T, Abe M, Kawamura T, Sasayama S. 2002. Rho/ROCK pathway contributes to the activation of extracellular signal-regulated kinase/GATA-4 during myocardial cell hypertrophy. J Biol Chem 277:8618–8625.